

Effect of Foundation Nonlinearity on Seismic Response of an Existing Arch Dam

P. Parsa Mahmoudi ^a, H. Mirzabozorg ^{b*}, M. Varmazyari ^c, S.M. Aghajanzadeh ^c

^a Graduate Student, Department of Civil Engineering, K. N. Toosi University of Technology, Tehran, Iran.

^b Associate Professor, Department of Civil Engineering, K. N. Toosi University of Technology, Tehran, Iran.

^c PhD Candidate, Department of Civil Engineering, K. N. Toosi University of Technology, Tehran, Iran.

Received 10 April 2016; Accepted 25 May 2016

Abstract

In the present paper, the effect of foundation nonlinearity on the seismic response of an existing arch dam is investigated. Luzzone arch dam in Switzerland is selected as a case study. The foundation nonlinearity is originated from opening/slipping of joints between a potential wedge at the left abutment and remaining foundation. Reservoir's water is assumed compressible and the coupled system is solved simultaneously. Also, the foundation is assumed massed medium via viscous boundary on the far-end truncated boundary. Two cases are considered in the analyses; the system applying reservoir pressure on the foundation; the system with no reservoir pressure applied on the foundation. The results reveal that the ignoring reservoir pressure on the foundation overestimates the response of the dam body. Finally, based on the conducted analyses, considering foundation nonlinearity has no significant effect on the results in the considered case due to special design of the body shape.

Keywords: Concrete Arch Dam; Foundation Nonlinearity; Massed Foundation; Seismic Analyses.

1. Introduction

The landslide sustained by some dam abutments i.e., Malpasset Dam in France and Vajont dam in Italy, altogether have attracted considerable research interest in the stability analysis of arch dams over past fifty years [1-4]. The safety evaluation of an arch dam should identify all factors in analyses to ensure that the structural stability of the dam is sustained. The stability of a concrete arch dam is strongly dependent on foundation and abutments on which the dam rests. In this regard, the stability against wedge sliding of arch dam-foundation has been subject of many researches. In 1965, Londe [5] proposed a fast approach to evaluate stability of rock wedges under thrust and uplift forces in dams. In 1999, Boyer and Ferguson [6] studied important factors to be considered in evaluating sliding stability of rock foundations for dams. Noble and Nuss [7] studied nonlinear seismic behaviour of Morrow Point dam considering a left abutment wedge. Their results revealed that the contraction joint openings are more severe when the wedge is not restricted or tied to the dam or foundation. At the same time, She [8] carried out numerical analysis of deformation and stability as well as effectiveness of the reinforcement at the right abutment of an arch dam. The results showed that the abutment might slide along the intersection of a fault. In 2005, Yu et al. [9] evaluated stabilities of sliding blocks on the abutments of a gravity arch dam by incorporating the results of finite element method analyses.

Some researchers have examined seismic responses of arch dams including rock wedges on the abutments by different approaches. Wang and Li [10] considered seismic responses of a high arch dam by experimental model. The system included the arch dam, contraction joints, and some parts of a reservoir, partial foundation and potential rock wedges on the abutments in which the mechanical properties including uplift on the kinematic planes were carefully simulated. In 2008, Mills-Bria et al. [11] investigated seismic nonlinear analyses of arch dams considering potential

* Corresponding author: mirzabozorg@kntu.ac.ir

block in the foundation using explicit finite element techniques.

Evaluating response of arch dam abutments to extreme loads such as earthquake has been conducted using static equilibrium equations approach like as Londe conventional method combined by finite element method [12]. Zenz et al. [13] investigated seismic stability of a rock wedge in the abutment of Luzzone dam. However, in their research the foundation was assumed as a massless medium. Takaloozadeh and Ghaemian [14] investigated Shape optimization of concrete arch dams considering abutment stability. The wedges in contact with the dam body were considered in their study. They concluded that considering abutment stability can change the optimum shape of arch dams and it is more important than tension stresses in the concrete arch dam body.

In the present paper, the effect of foundation nonlinearity on the seismic response of an existing arch dam is investigated. Luzzone arch dam in Switzerland is selected as the case study. The foundation nonlinearity is originated from opening/slipping of joints between a potential wedge at the left abutment and remaining foundation. Reservoir's water is assumed compressible and the coupled system is solved simultaneously. Also, the foundation is assumed massed medium via viscous boundary on the far-end truncated boundary. Two cases are considered in the analyses; the system including reservoir pressure on the foundation; the system with no reservoir pressure applied.

2. Finite Element Models

2.1. Foundation Interaction and Wave Propagation

The equations governing the P and S wave propagation within the massed foundation rock are given as:

$$\frac{\partial^2 \mathbf{u}}{\partial t^2} = V_p^2 \nabla^2 \mathbf{u} \quad (1)$$

$$\frac{\partial^2 \mathbf{v}}{\partial t^2} = V_s^2 \nabla^2 \mathbf{v} \quad (2)$$

$$\frac{\partial^2 \mathbf{w}}{\partial t^2} = V_s^2 \nabla^2 \mathbf{w} \quad (3)$$

in which, u , v and w are displacements in the direction of wave propagation and the two other orthogonal directions, respectively and V_p and V_s are primary and secondary wave propagation velocities within the rock medium given as:

$$V_p = \sqrt{\frac{E_r (1 - \nu_r)}{\rho_r (1 + \nu_r) (1 - 2\nu_r)}} \quad (4)$$

$$V_s = \sqrt{\frac{G_r}{\rho_r}} = \sqrt{\frac{E_r}{2 (1 + \nu_r) \rho_r}} \quad (5)$$

where, E , G , ν and ρ are the modulus of elasticity, shear modulus, Poisson's ratio and density, respectively and subscript r indicates that the parameters are pertinent to the foundation rock. One of the main aspects in the seismic loading and wave propagation within the semi-infinite medium such as the rock underlying structures is preventing the wave reflection from the artificial boundary on the far end nodes into the provided finite element model. In this study an appropriate viscous boundary, which is a non-consistent boundary is applied on the far-end boundary of the foundation in 3D space expressed as [15]:

$$\sigma = \rho_r V_p \dot{u} \quad (6)$$

$$\tau_1 = \rho_r V_s \dot{v} \quad (7)$$

$$\tau_2 = \rho_r V_s \dot{w} \quad (8)$$

Where, σ , τ_1 and τ_2 are the normal and two in-plane shear stresses in global directions, and u , v and w are the normal and two tangential displacements, respectively.

Radiation damping derived from Equations (6)-(8) applied on the far-end boundary of the foundation is made up of dashpots that are added to the global damping matrix of the structure, $\{C\}$. In the present research, these lumped dashpots are determined as [15]:

$$C_{11}^i = V_p \rho_r \int_{A_c} N_i dA \quad (9)$$

$$C_{22}^i = V_s \rho_r \int_{A_c} N_i dA \quad (10)$$

$$C_{33}^i = V_s \rho_r \int_{A_e} N_i dA \tag{11}$$

where, C_{11}^i , C_{22}^i and C_{33}^i are components of lumped damping applied on the i^{th} node of the surface element on the far end boundary of the surrounding rock in normal and two orthogonal tangential directions, respectively; N_i is the i^{th} node shape function; and all the integrations are applied over the area of the considered surface of the element, A_e .

2.2. Rock Joint Modeling

In the present study, for modeling joints a special contact element is used which is able to model contact between two adjacent nodes in 3D domain. This contact element supports compression in normal direction and shear in the tangential direction. Figure 1. shows the flowchart used for calculating force in contact elements in which V is a vector representing contact state, V_n indicates the state in the normal direction to the plane of the joint, and V_r and V_s indicate the state of the considered contact element in tangential directions. Moreover, Figure 2. shows force deflection relations for both normal and tangential status. In this flowchart F_n , F_r and F_s are local components of force vector; F_g is sliding force in the joint; F_t is shear force resultant in the joint; K_n and K_t are normal and tangential stiffness of the joint and α is the angle between the two components of in-plane shears. As shown, contact element cannot endure any tensile force or stress, but when it is in compression, it can suffer compression forces according to its normal stiffness and shear forces according to the tangential stiffness. When shear force resultant in the joint exceeds the joint sliding resisting force, the two nodes of the element begin sliding with respect of each other. Joint sliding force is calculated using coulomb friction law. In Figure 1, c is cohesion factor and μ is friction coefficient [16].

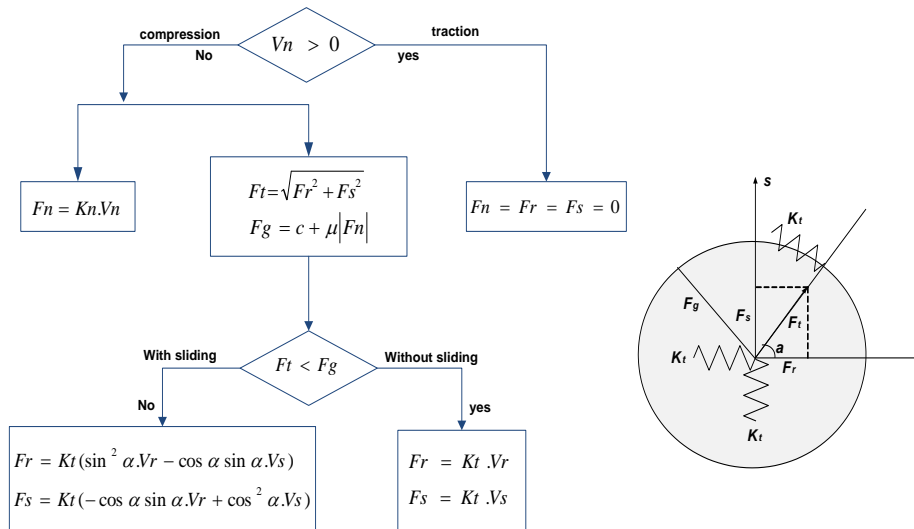


Figure 1. Flowchart for calculating force in joints [16]

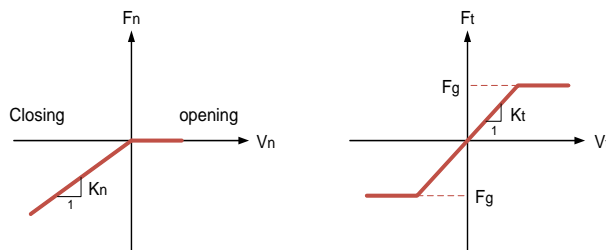


Figure 1. Force-deflection relations for joint; (a) Normal opening; (b) Tangential movement [16]

2.3. Fluid-Structure-Interaction

Considering the coupled dam-reservoir-foundation system, the governing equation in the reservoir medium is Helmholtz given as [17-18]:

$$\nabla^2 p = \frac{1}{C^2} \frac{\partial^2 p}{\partial t^2} \tag{12}$$

Where p , C , and t are the hydrodynamic pressure, pressure wave velocity in liquid domain, and time, respectively. Boundary conditions, which should be applied on the reservoir medium to solve Equation (12) can be found in [16-

17]. The governing equations on the dam-foundation (as the structure) and the reservoir take the following form:

$$\begin{bmatrix} [M] & 0 \\ \rho[Q]^T & [G] \end{bmatrix} \begin{Bmatrix} \ddot{U} \\ \ddot{P} \end{Bmatrix} + \begin{bmatrix} [C] & 0 \\ 0 & [C'] \end{bmatrix} \begin{Bmatrix} \dot{U} \\ \dot{P} \end{Bmatrix} + \begin{bmatrix} [K] & -[Q] \\ 0 & [K'] \end{bmatrix} \begin{Bmatrix} U \\ P \end{Bmatrix} = \begin{Bmatrix} \{f_1\} - [M]\{\ddot{U}_g\} \\ \{F\} - \rho[Q]^T\{\ddot{U}_g\} \end{Bmatrix} \quad (13)$$

Where, $[M]$, $[C]$ and $[K]$ are the mass, damping and stiffness matrices of the structure including the dam body and its surrounding foundation rock and $[G]$, $[C']$ and $[K']$ are matrices representing the mass, damping and stiffness equivalent matrices of the reservoir, respectively. The matrix $[Q]$ is the coupling matrix; $\{f_1\}$ is the vector including both the body and the hydrostatic force; $\{P\}$ and $\{U\}$ are the vectors of hydrodynamic pressures and displacements, respectively and $\{\ddot{U}_g\}$ is the ground acceleration vector.

3. Luzzone Dam as Case Study

Luzzone dam is a 225 m high double curvature arch dam located in south-eastern of Switzerland. The dam was built in 1960 and it was heightened with 17 meters in 1990. Its maximum thickness at the base is 36 m (Figure 3). The finite element model provided for the dam, surrounding rock soil and water is presented in Figure 4. The model consists of 316 8-node solid elements for modeling concrete dam and '3299' 8-node solid elements for modeling the surrounding foundation rock. The utilized 8-node solid elements have three translational degrees of freedom at each node. In addition, water is modeled using '945' 8-node fluid elements having three translational DOFs and one pressure DOF in each node. It should be noted that translational DOFs are active only at nodes that are on the interface with solid elements. Material properties for mass concrete and foundation are described in Table 1 [12]. Reservoir water density is 1000 Kg/m^3 and the sound velocity in water is taken as 1440 m/s . Also, wave reflection coefficient for reservoir around boundary is assumed 0.8, conservatively.

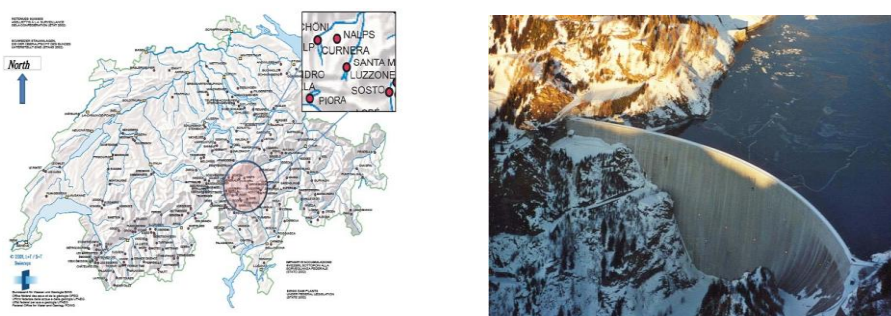


Figure 3. Overall view of Luzzone dam and its location [12]

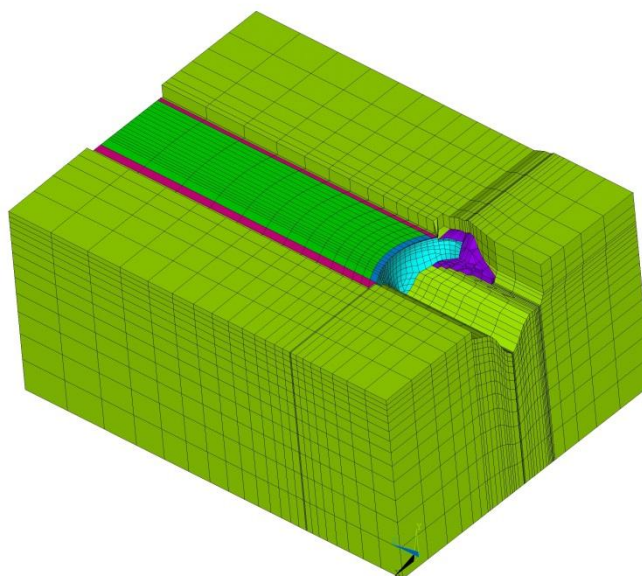


Figure 4. Finite element model of dam reservoir foundation system

Table 1. Material property of the mass concrete dam and foundation [12]

Label	Dam	Foundation
E (GPa)	27	25
ρ (Kg/m ³)	2400	2600
ν_{concrete}	0.17	0.2
Mass damping coefficients, α	0.6	0.6
Stiffness damping coefficients, β	0.001	0.001

3.1. Wedge Definition

During the construction, some set of decompressed joint structures on the left bank opened and provoked an instability which had important consequences on the geometrical definition of the dam and stability of the abutments. These decompressed diabase rock formations were predominant on the left bank as was evident from the relatively large seepages observed on the left bank as compared to the right bank. Geological joints present a potential wedge (Figure 4) to sliding that a stability evaluation is necessary here. The volume of the wedge is estimated to be 1.92 mcm. The wedge position is delimited by three planes. Downstream view of the wedge is shown in Figure 5. (see Figure 4).

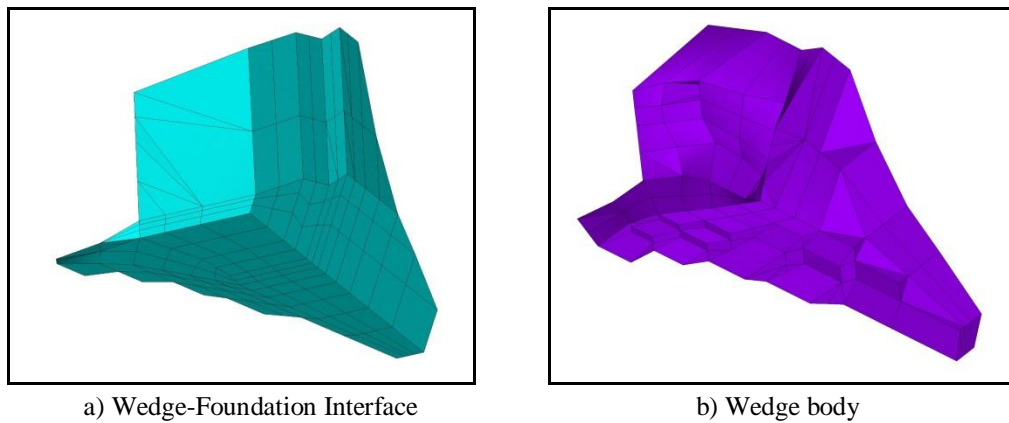


Figure 5. Downstream view of the wedge

3.2. Seismic Data

For seismic analysis, three stochastically independent acceleration time-histories pertinent to the site are applied to the system at the foundation boundaries, simultaneously (Figure 6). The peak ground accelerations in the cross valley, vertical and upstream-downstream directions are 0.12 g, 0.093 g and 0.092 g, respectively [12].

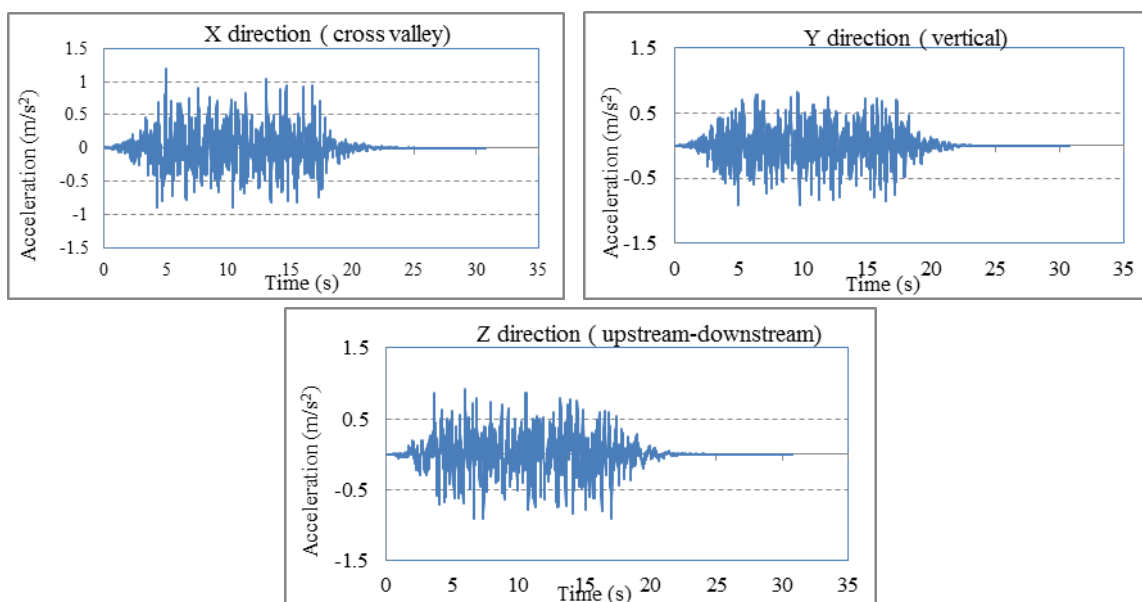


Figure 6. Three components of the Switzerland earthquake [12]

4. Displacement Results

4.1. Foundation Nonlinearity Effect

Figure 7. shows the crest displacement in stream direction extracted from conducted analyses for the cases of linear and nonlinear foundation. Figure 8. shows the results when reservoir weight is applied on the foundation. As shown in the figures, there is no difference between both models. This can be due to the fact that the only upstream face of the dam body is in contact with the wedge and the design of dam body shape in this region is excellent.

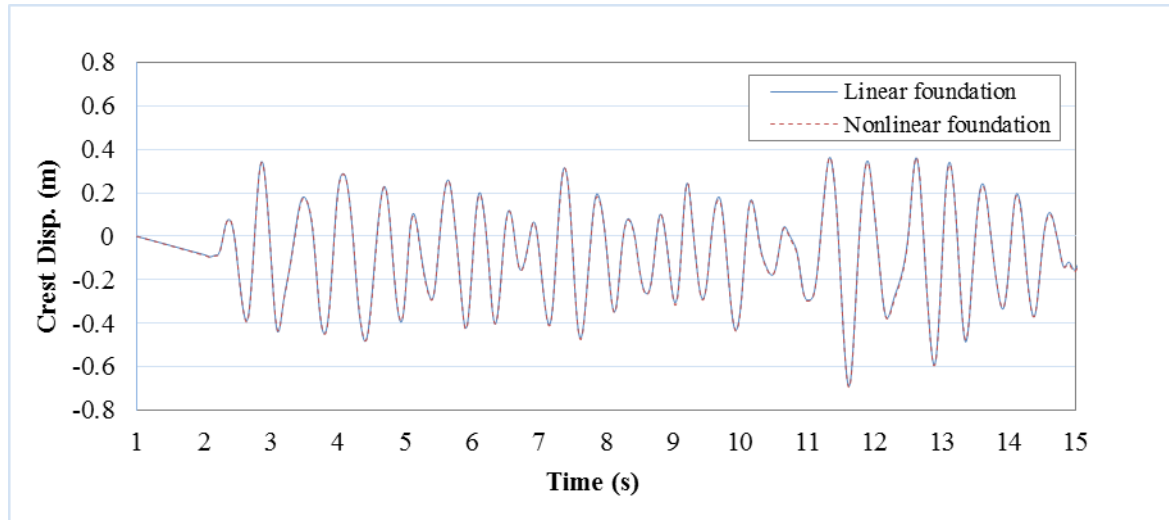


Figure 7. Crest displacement in upstream-downstream direction with no reservoir pressure applied: linear foundation; nonlinear foundation

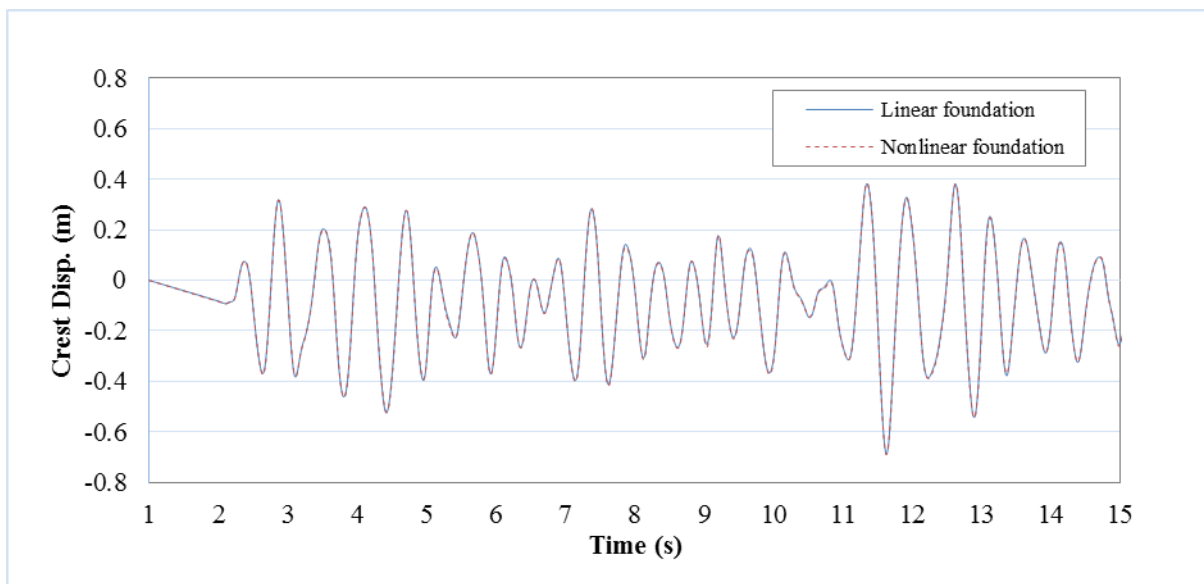


Figure 8. Crest displacement in upstream-downstream direction with reservoir pressure applied: linear foundation; nonlinear foundation

Figures 9. compares the wedge displacements in upstream-downstream direction when the reservoir pressure is applied on the nonlinear foundation to that of the model with no reservoir pressure applied. As shown in the figures, the frequency content is the same for both models but the applying reservoir pressure on the foundation leads to less crest displacement. The figures for linear foundation model are shown in Figure 10. When the reservoir pressure is applied on the nonlinear foundation, the crest displacements in upstream and downstream directions are decreased at most by 29% and 22%, respectively, in comparison with the model in which no reservoir pressure is applied. These values reach to 31% and 22% when no contact element is applied between the wedge and the remaining foundation. It is worth noting that when the pressure of the reservoir is applied, the rigidity of the dam body is increased due to foundation and abutments deformations.

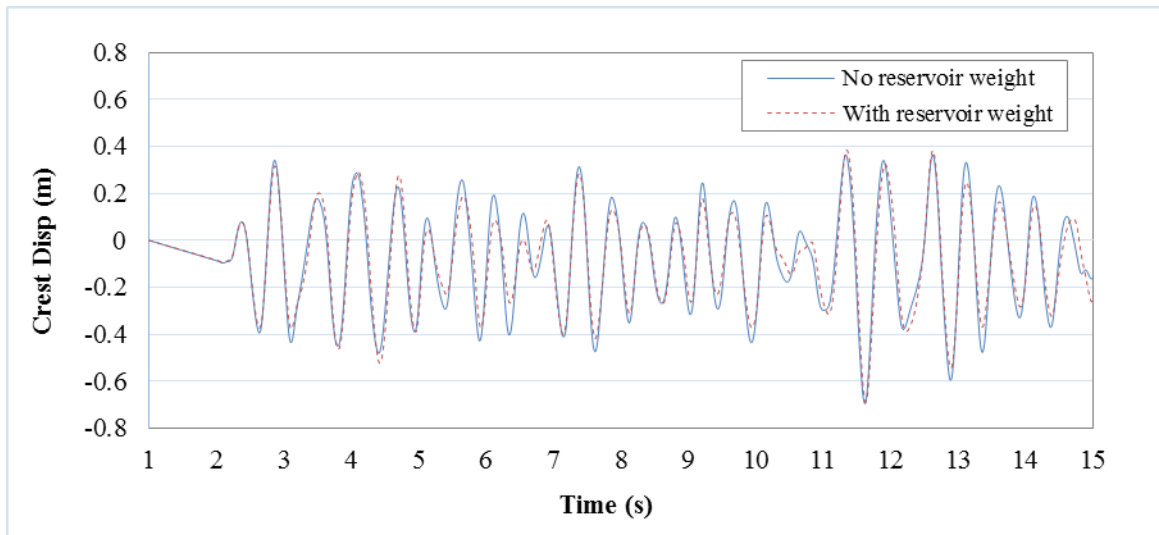


Figure 9. Crest displacement in upstream-downstream direction considering nonlinear foundation: applying reservoir pressure; applying no reservoir pressure

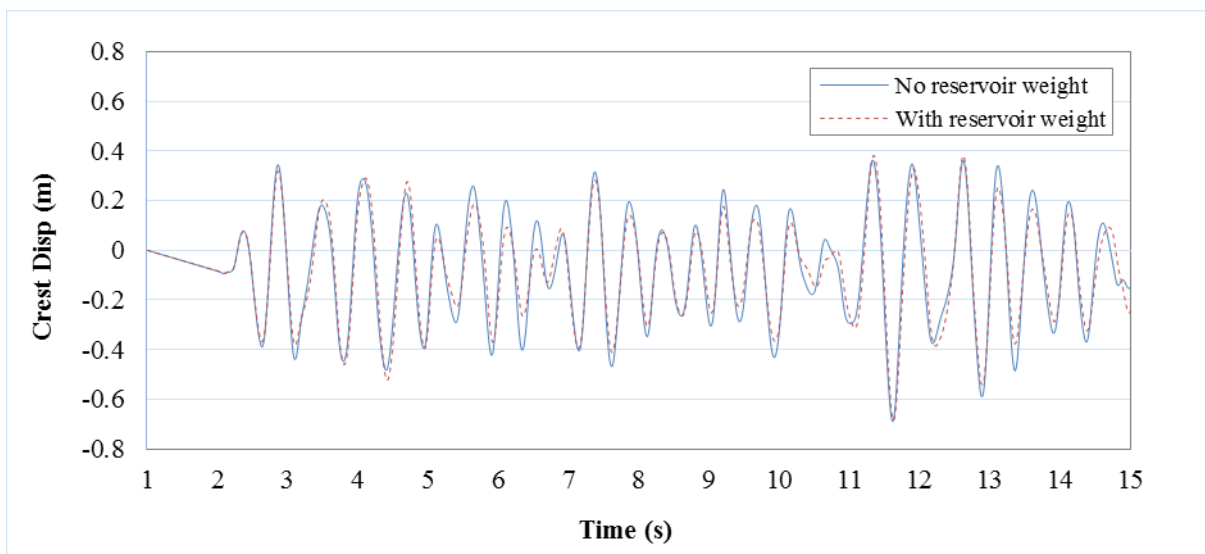


Figure 10. Crest displacement in upstream-downstream direction considering linear foundation: applying reservoir pressure; applying no reservoir pressure

5. Stress Results

Figures 11 to 14 present non-concurrent envelope of the first and third principal stresses within the dam body for various conditions of the foundation and reservoir. As can be seen, the foundation nonlinearity causes no significant change in the stress levels. It is worth noting that the dam was constructed geometrically to minimize the impact of wedge sliding on the stability of the dam body. In addition, comparing Figures 11 and 13 to Figures 12 and 14 it can be observed that applying reservoir pressure on the foundation decrease stresses slightly. Finally, Table 2 summarizes maximum values of tensile and compressive stresses within the dam body for various conditions of the foundation and reservoir pressure application way.

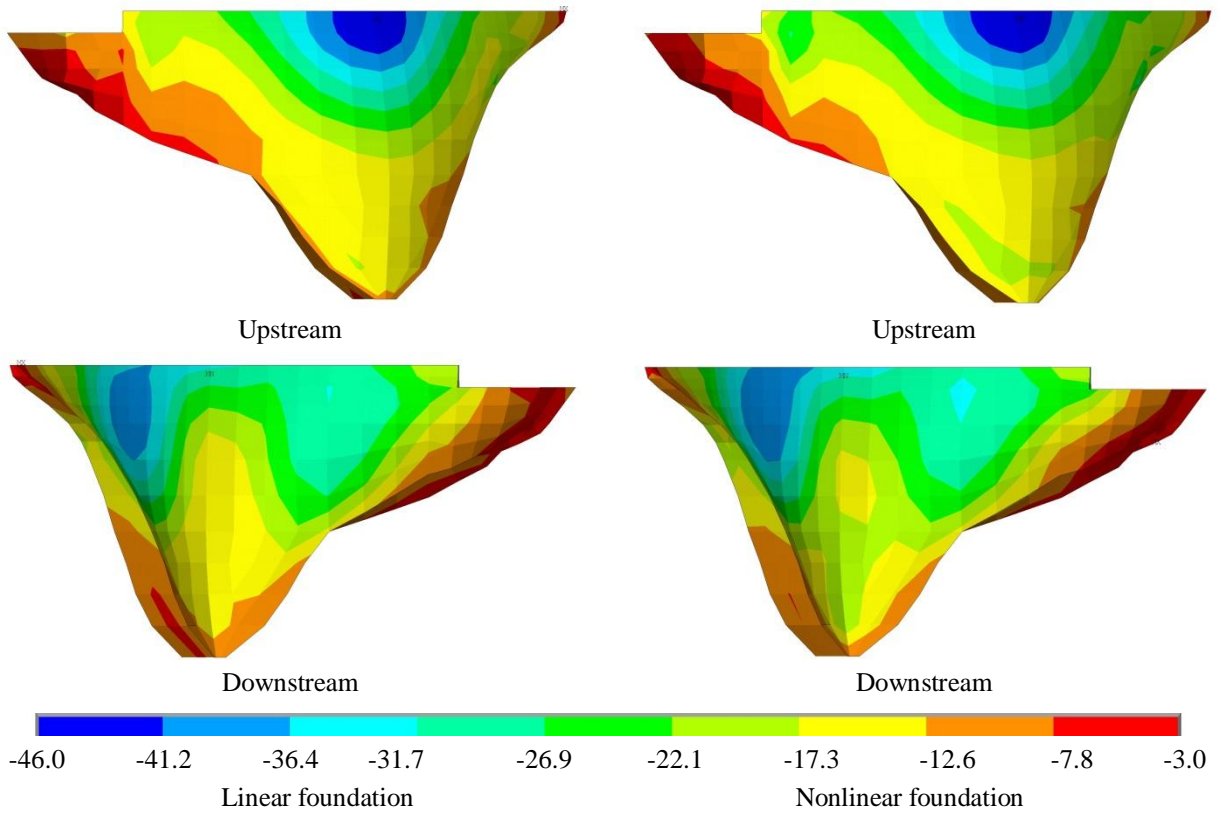


Figure 11. Non-concurrent envelope of the third principal stress on upstream and downstream faces for nonlinear and linear foundation; No applying reservoir pressure

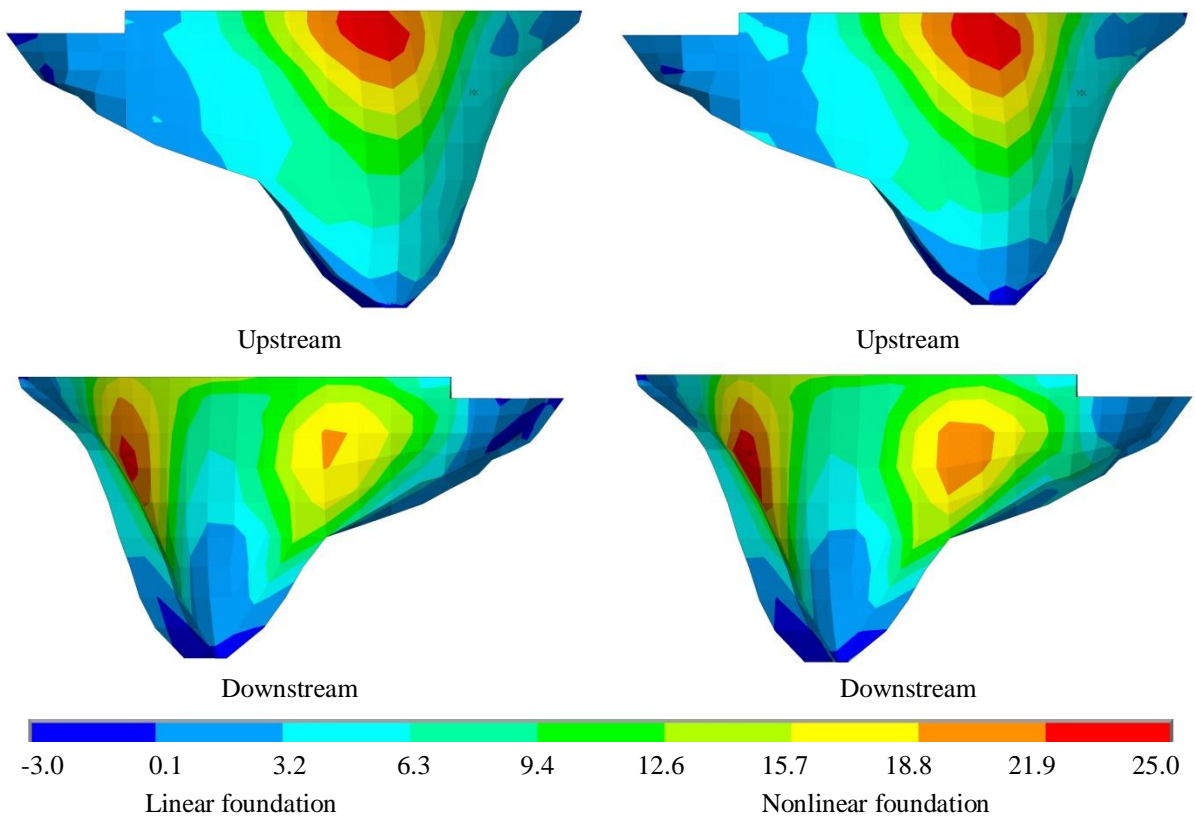


Figure 12. Non-concurrent envelope of the first principal stress on upstream and downstream faces for nonlinear and linear foundation; No applying reservoir pressure

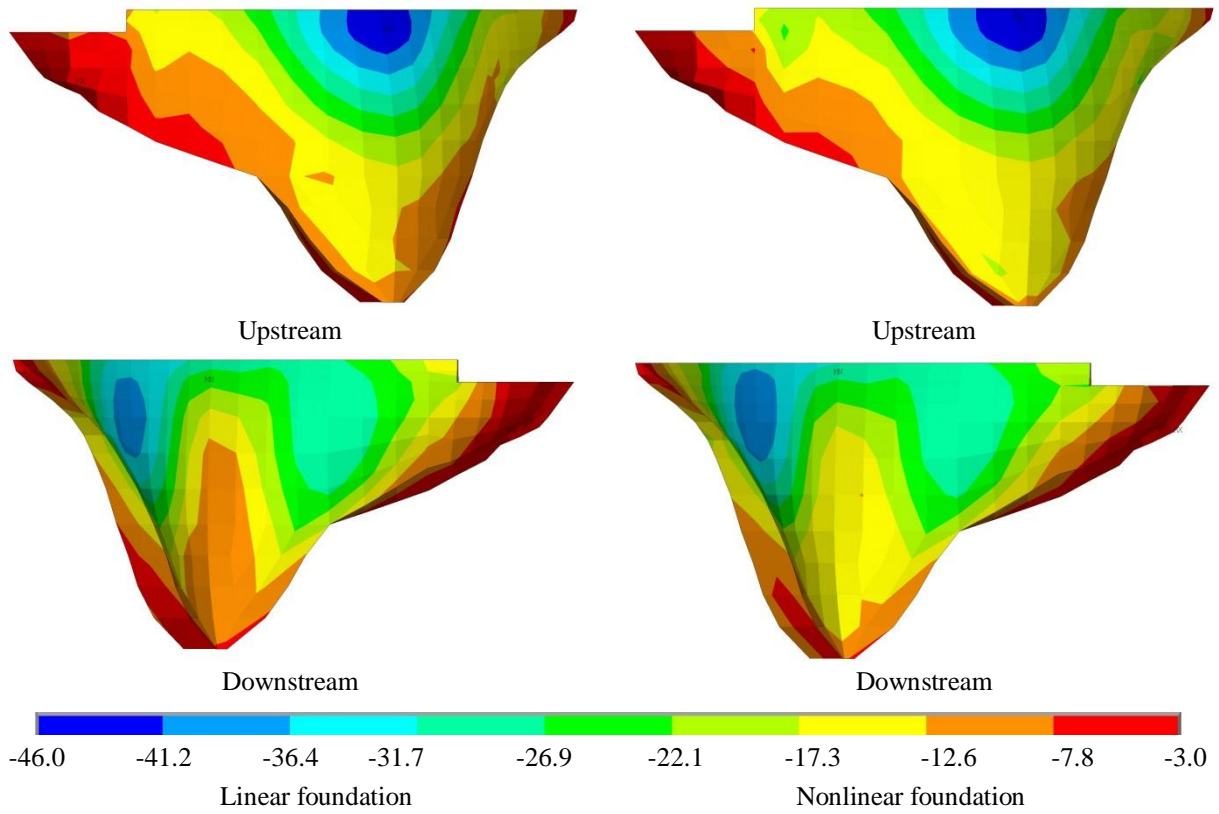


Figure 13. Non-concurrent envelope of the third principal stress on upstream and downstream faces for nonlinear and linear foundation; with applying reservoir pressure

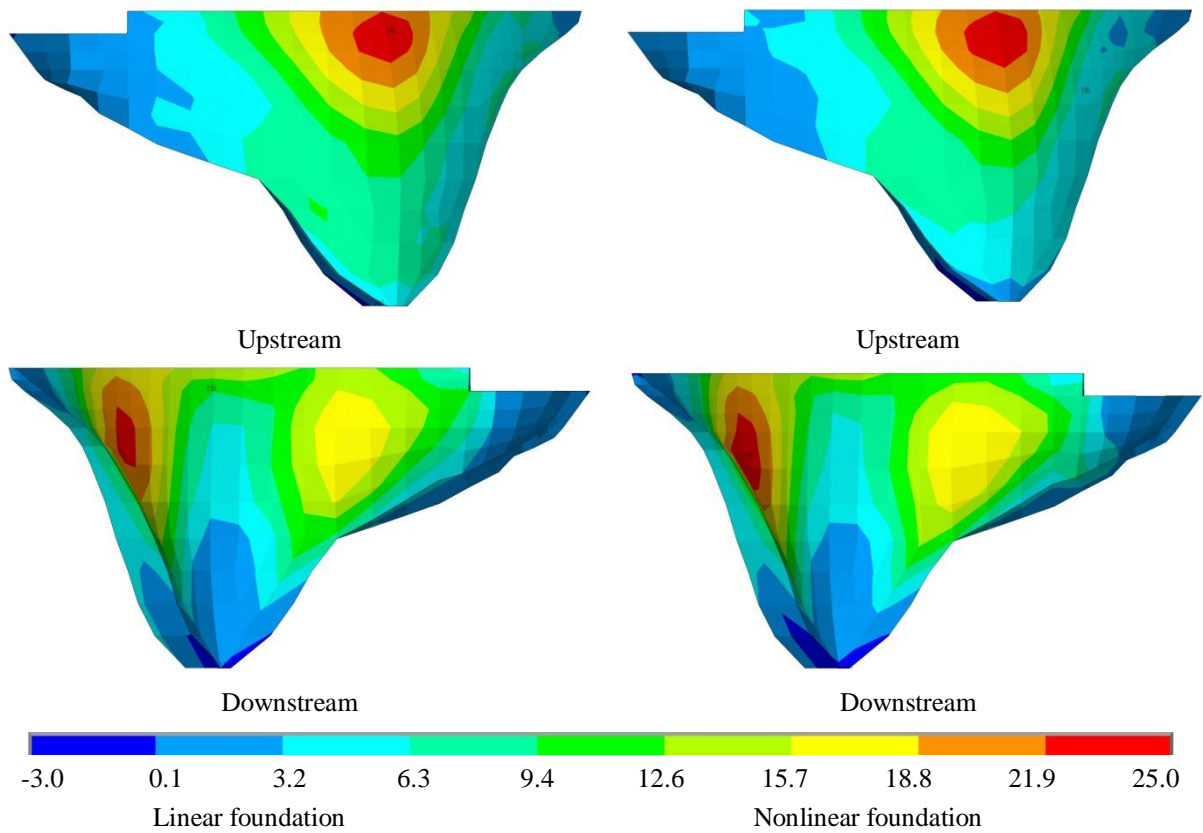


Figure 14. Non-concurrent envelope of the first principal stress on upstream and downstream faces for nonlinear and linear foundation; with applying reservoir pressure

Table 2. Maximum values of tensile and compressive stresses within the dam body for various conditions of foundation and reservoir

Stress	Foundation State	Values (MPa)	
		No reservoir weight	Applied reservoir weight
Compressive	Nonlinear (Joint)	-45.9	-44.7
	Linear	-45.5	-44.5
Tensile	Nonlinear (Joint)	24.9	24.3
	Linear	23.8	23.8

6. Conclusion

In the present paper, the effect of foundation nonlinearity on the seismic response of an existing arch dam is investigated. Luzzone arch dam in Switzerland is selected as a case study. The foundation nonlinearity is originated from opening/slipping of joints between a potential wedge at the left abutment and remaining foundation. Reservoir's water is assumed compressible and the coupled system is solved simultaneously. Also, the foundation is assumed massed applying an appropriate viscous boundary on it's the far-end truncated around. Two cases are considered in the analyses; the system applying reservoir pressure on the foundation around interfacing with the reservoir located in the upstream; the system with no applied reservoir pressure on the foundation. Based on the conducted analyses, considering foundation nonlinearity has no significant effect on the results due to excellent geometric design of the dam body in vicinity of the left abutment. In addition, it is observed that applying reservoir pressure on the foundation located in the upstream leads to less response of the system which is much more realistic result in dam safety evaluation. At last, it is worth noting that uncertainties associated with some parameters of the wedge stability such as sliding surface require further studies.

7. References

- [1] Londe, P. The Malpasset dam failure. *Engineering Geology* 24.1 (1987): 295-329.
- [2] Wittke, W., and G. A. Leonards. Modified hypothesis for failure of the Malpasset Dam. *Engineering Geology* 24.1 (1987): 407-421.
- [3] Kottenstette, J. T. Block theory techniques used in arch dam foundation stability analysis. *International Journal of Rock Mechanics and Mining Sciences* 34.3 (1997): 163-e1.
- [4] Jun-rui, C. H. A. I. Review on Dynamic Stability Analysis of Rock Mass in High Arch Dam Abutment. *Journal of Liaoning Technical University (Natural Science Edition)* 4 (2001): 042.
- [5] Londe, P., Analysis of the stability of rock slopes. *Quarterly Journal of Hydrogeology* 6, 93-124 (1973).
- [6] Boyer, D.D. and Ferguson, K.A. Important factors to consider in evaluating sliding stability of rock foundations for dams. 16th Annual Conference: Association of State Dam Safety Officials (ASDSO), October 10-13, 1999. ST. Louis, US.
- [7] Noble, Charles R., and Nuss, Larry K.. Nonlinear seismic analysis of Morrow Point dam. 13th World Conference on Earthquake Engineering Vancouver, Canada, 1-6, August 2004.
- [8] She, C. X. Deformation and stability of the right arch dam abutment of the Danjiang Hydro-Power project, China. *International Journal of Rock Mechanics and Mining Sciences*, 41 (2004): 792-797.
- [9] Yu, X., Zhou Y. F., and Peng S. Z. Stability analyses of dam abutments by 3D elasto-plastic finite-element method: a case study of Houhe gravity-arch dam in China. *International journal of rock mechanics and mining sciences*. 42.3 (2005): 415-430.
- [10] Wang, Haibo, and Deyu Li. Experimental study of dynamic damage of an arch dam. *Earthquake engineering & structural dynamics*, 36.3 (2007): 347-366.
- [11] Mills-Bria, Barbara L., Nuss, Larry K.; Chopra, Anil K. Current methodology at the Bureau of Reclamation for the nonlinear analyses of arch dams using explicit finite element techniques. The 14th World Conference on Earthquake Engineering October 12-17, 2008, Beijing, China
- [12] Sohrabi Gilani M., Feldbacher R. and Zenz G., Stability of dam abutment including seismic loading. 10th Benchmark Workshop on Numerical Analysis of Dam, ICOLD, Paris, France, 16-18 September, (2009).
- [13] Zenz G., Goldgruber M. and Feldbacher R., Seismic stability of a rock wedge in the abutment of an arch dam, *Geomechanics and Tunneling*, 5, 186-194 (2012).
- [14] Takaloozadeh M. and Ghaemian M. Shape optimization of concrete arch dams considering abutment stability. *Scientia Iranica A* (2014) 21(4), 1297-1308
- [15] Mirzabozorg H., Kordzadeh A. and Hariri Ardebili M. A., Seismic response of concrete arch dams including dam-reservoir-foundation interaction using infinite elements, *Electronic Journal of Structural Engineering*, 12, 63-73 (2012).

- [16] Hariri Ardebili M. A. and Mirzabozorg H., Investigation of endurance time method capability in seismic performance evaluation of concrete arch dams, *Dam Engineering*, 22, 35-64 (2011).
- [17] Mirzabozorg H., Khaloo A. R. and Ghaemian M., Staggered solution scheme for three-dimensional analysis of dam-reservoir interaction, *Dam Engineering*, 14, 1-33 (2003).
- [18] Mirzabozorg H. and Ghaemian M., Nonlinear behavior of mass concrete in three-dimensional problems using smeared crack approach, *Earthq Eng Struct Dyn*, 34, 247-269 (2005).
- [19] Westergaard H. M., Water pressures on dams during earthquakes, *Trans. ASCE*, 98, 418-433 (1933).